ChemPubSoc Europe

DOI: 10.1002/chem.201402709

CHEMISTRY A European Journal Full Paper

Dendrimers

A New Class of Tunable Dendritic Diphosphine Ligands: Synthesis and Applications in the Ru-Catalyzed Asymmetric Hydrogenation of Functionalized Ketones

Baode Ma,[a] Tingting Miao,[a] Yihua Sun,[b] Yanmei He,[a] Ji Liu,[a] Yu Feng,[a] Hui Chen,*[b] and Qing-Hua Fan*[a]

Abstract: A series of tunable G_0–G_3 dendritic 2,2′-bis(diphenylphosphino)-1,1′-binaphthyl (BINAP) ligands was prepared by attaching polyaryl ether dendrons onto the four phenyl rings on the P atoms. Their ruthenium complexes were employed in the asymmetric hydrogenation of β-ketoesters, α-ketoesters, and α-ketoamides to reveal the effects of dendron size on the catalytic properties. The second- and third-generation catalysts exhibited excellent enantioselectivities, which are remarkably higher than those obtained from the small molecular catalysts and the first-generation catalyst. Molecular modeling indicates that the incorporation of bulky dendritic wedges can influence the steric environments around the metal center. In addition, the ruthenium catalyst bearing a second-generation dendritic ligand could be recycled and reused seven times without any obvious decrease in enantioselectivity.

Introduction

Dendrimers are fascinating man-made macromolecules owing to their unique physical and chemical properties,[1] and have been served as a new class of catalyst supports.[2] Unlike the traditional cross-linked polymer-supported catalysts, dendrimer catalysts possess well-defined molecular architectures with nanoscale size.[3] They catalyze the reaction under homogeneous manner, and can be easily recycled at the end of reaction by solvent precipitation or nanofiltration. Therefore, the dendrimer catalyst offers a unique potential to combine the advantages of both homogeneous catalysis and conventional heterogeneous catalysis. To date, lots of organometallic dendrimers bearing catalytically active units at the core and/or at the periphery have been described.[2,4–6] However, only a few dendrimer catalysts, particularly, chiral dendrimer catalysts have shown a "positive dendrimer effect", which is referred to when the reactivity and/or stereoselectivity of the dendritic catalyst increases in comparison with the parent catalyst.[3,7,8] This can be attributed to a cooperative interaction of two or more catalytic sites at the periphery or an isolation effect of catalytic site at the core.

For asymmetric catalysis, subtle changes in conformational, steric and/or electronic properties of the chiral ligands can often lead to dramatic variations of reactivity and enantioselectivity.[9] Thus, attachment of the well-defined and bulky dendritic wedges onto the framework of a chiral catalyst is expected to provide a unique tool for fine-tuning the enantioselectivity.[10] For example, we recently reported chiral dendritic monodentate phosphoramidite ligands by replacing both methyl groups on the N atom of the phosphoramidite ligand with different generation polyether dendritic wedges.[8f] Their rhodium complexes exhibited unprecedentedly increased enantioselectivity upon using higher-generation dendrimers in the asymmetric hydrogenation of α-dehydroamino acid derivatives and enamides. As an extension of our research on chiral dendrimer catalysts and our continued interests in the development of recyclable catalysts,[3,11] here we wish to report a new class of tunable and recylable dendritic chiral diphosphine ligands.

The design and synthesis of chiral diphosphine ligands have played a significant role in the development of efficient transition-metal-catalyzed asymmetric hydrogenations.[12] Among the reported various chiral diphosphine ligands, most of them involve a chiral skeleton bearing two diphenylphosphine chelating units. The chiral information is transferred from the chiral skeleton to the catalytically active metal center through the chiral array of the four phenyl rings at the P atoms.[13] Further modifications to the chiral skeleton and/or the chelating units by introducing small molecular substituents with different steric and/or electronic properties are often used strategy to fine-tune the chiral microenvironment around the metal center. On the basis of this method, some conformationally

[a] Dr. B. Ma, T. Miao, Y. He, Dr. J. Liu, Dr. Y. Feng, Prof. Dr. Q.-H. Fan
Beijing National Laboratory for Molecular Sciences
and CAS Key Laboratory of Molecular Recognition and Function
Institute of Chemistry, Chinese Academy of Sciences (CAS)
Beijing 100190 (P.R. China)
E-mail: fanqh@iccas.ac.cn

[b] Y. Sun, Prof. Dr. H. Chen
Beijing National Laboratory for Molecular Sciences
and CAS Key Laboratory of Photochemistry
Institute of Chemistry, CAS, Beijing 100190 (P.R. China)
E-mail: chenh@iccas.ac.cn

Supporting information for this article is available on the WWW under http://dx.doi.org/10.1002/chem.201402709.

rigid and yet tunable ligands have been reported and demonstrated excellent asymmetric induction in transition-metal-catalyzed asymmetric hydrogenation reactions.[14] However, most homogeneous catalytic systems suffer from difficulty in separation and recycling of the expensive chiral catalyst.[11,15] It is still a big challenge to develop ideal chiral catalysts possessing excellent catalytic ability and easy recyclability.[3]

Considering the well-defined and nanoscale dendritic architectures, here we report a new general method to modify the chiral diphosphine ligands by attaching sterically demanding dendritic wedges onto the four phenyl rings at the P atoms.[16,17] In addition to the specific microenvironment created by the branched dendritic shell, the increasing steric repulsion between the four larger dendritic wedges with the increase of generation can influence the chiral array of the four phenyl rings, and consequently modulate and improve the catalytic behavior of the core. To exemplify our approach, we chose BINAP as the model diphosphine ligand for this study.[18] A series of dendritic BINAP ligands bearing polyether dendrons at the *para* position of the four phenyl rings on the P atoms were synthesized. Their ruthenium complexes proved to be effective catalysts in the asymmetric hydrogenation of β-ketoesters, α-ketoesters, as well as the less-explored α-ketoamides. The size of the dendritic wedges was found to be crucial in achieving high asymmetric induction. Remarkably higher enantioselectivities with higher-generation catalysts were observed compared with those of the small molecular and the low-generation catalysts. In addition, the dendrimer catalyst could be easily recycled several times by solvent precipitation without obvious decrease of enantioselectivity.

Results and Discussion

Synthesis of dendritic BINAP ligands and their ruthenium complexes

Fréchet-type polyaryl ether dendrons were chosen for this study due to their inertness to reaction and inability to coordinate metal, as well as easy preparation.[19] The synthesis and structures of the dendritic ligands are shown in Scheme 1. By using a convergent strategy, the first to third generation BINAP-cored dendrimers were synthesized by coupling (*R*)-**OH-BINAPO** with the corresponding dendritic wedges **G_n-Br** followed by reduction of **G_n-BINAPO** with $HSiCl_3/N(n\text{-}Bu)_3$,[20] providing the target dendritic ligands (*R*)-**G_n-BINAP** in quite good yields. It is worth mentioning that all the dendritic intermediates and final ligands could be purified by solvent precipitation method without the use of column chromatography. For comparison, two small molecular BINAP derivatives **MeO-BINAP** and **G_0-BINAP** were also synthesized. All these BINAP ligands

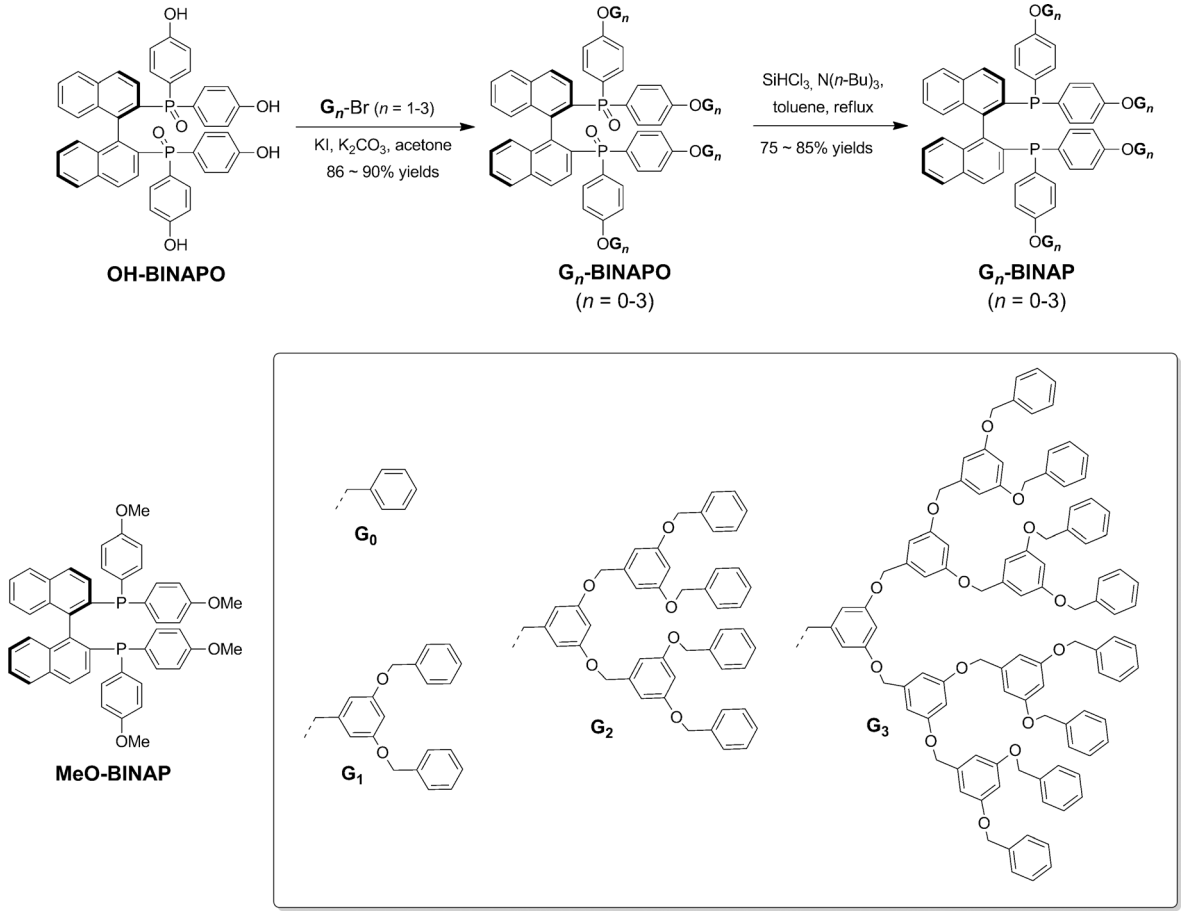

Scheme 1. Synthesis and molecular structures of chiral dendritic BINAP ligands.

were well characterized by ^{1}H, ^{13}C, and ^{31}P NMR spectroscopy, MALDI-TOF mass spectrometry and elemental analysis. All the results were consistent with the compounds synthesized.

With these dendritic BINAP ligands in hand, we prepared their ruthenium complexes by mixing the corresponding dendritic ligands with [RuI_2(*p*-cymene)] in a mixture of CH_2Cl_2 and CH_3OH at room temperature for 60 min under nitrogen atmosphere. The solvent was then removed under reduced pressure to give the in situ dendritic catalysts as orange powders. The chemical shifts of all these ruthenium complexes were very similar ($\delta \approx 36$ and ≈ 19 ppm, $J_{pp} = \approx 60$ Hz), indicating that the introduction of sterically demanding dendritic wedges could not influence the coordination of ruthenium with the phosphorus atoms at the core of the dendrimer, as shown in Figure 1. Notably, all dendritic catalysts are well soluble in CH_2Cl_2, THF, and toluene, whereas the second- and third-generation catalysts are practically insoluble in methanol. The different solubility of the dendritic catalysts thus offered a reliable method for subsequent separation and recycling of the ruthenium catalysts.

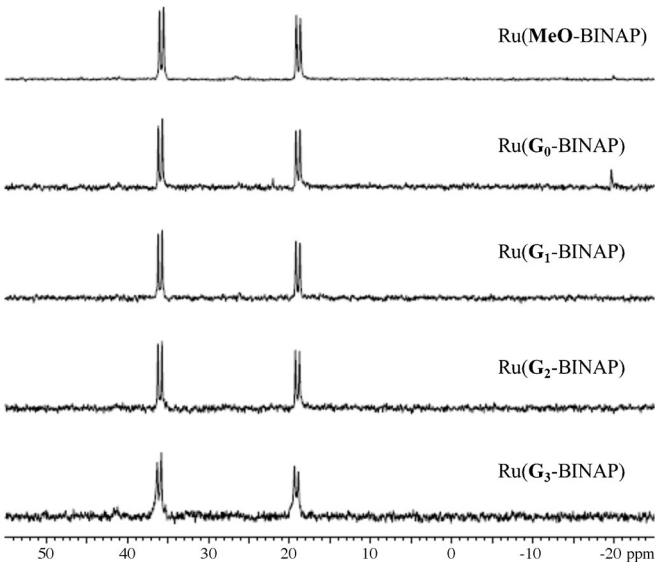

Figure 1. ^{31}P NMR spectra of dendritic [Ru(**G$_n$-BINAP**)] complexes and corresponding small molecular Ru catalysts.

Asymmetric hydrogenation of β-ketoesters

Asymmetric hydrogenation of β-alkyl- and β-aryl β-ketoesters provides a direct approach to optically active β-hydroxy acids and their derivatives,[12,21] which are very important structural motifs in numerous biologically compounds.[22] Accordingly, a number of chiral diphosphine ligands have been developed for the Ru-catalyzed asymmetric hydrogenation of β-ketoesters. However, only a few of them exhibited high asymmetric induction for the hydrogenation of β-aryl β-ketoesters.[14c,23] As an example, Noyori and co-workers pioneeringly reported a highly asymmetric hydrogenation of β-alkyl β-ketoesters by using the Ru-BINAP system, but much more inferior enantioselectivities were obtained for analogous β-aryl ketoester substrates.[24] To evaluate the efficiency of the dendritic [Ru(**G$_n$-BINAP**)] complexes and to established the relationship between the size of the dendrimer and its catalytic properties, the Ru-catalyzed asymmetric hydrogenation of β-ketoesters was chosen as the model reaction.

As shown in Table 1, all these ruthenium catalysts were effective in the asymmetric hydrogenation of both β-alkyl- and β-aryl β-ketoester substrates, and an unusual dendrimer effect was observed. For example, the hydrogenation of methyl 4-(benzyloxy)-3-oxobutanoate proceeded smoothly in the presence of 0.2 mol% catalyst. The size of substituents on phenyl rings of the P atoms was found to influence the enantioselectivity remarkably (entry 1, Table 1). The zeroth- and first-generation catalysts gave the reduced product with enantiomeric excesses

Table 1. Asymmetric hydrogenation of β-ketoesters with dendritic [Ru(BINAP)].[a]

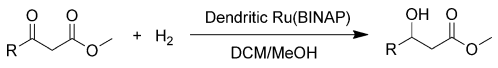

Entry	Substrate	Conversion [%];[b] *ee* [%][c] MeO-BINAP	G_0-BINAP	G_1-BINAP	G_2-BINAP	G_3-BINAP
1	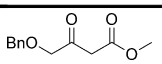	>95; 84	>95; 66	>95; 44	>95; 92	>95; 97
2	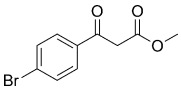	>95; 83	>95; 67	>95; 54	>95; 95	>95; 97
3	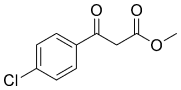	>95; 82	>95; 69	>95; 42	>95; 92	67; 92
4	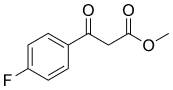	>95; 82	>95; 64	>95; 50	67; 93	33; 94
5	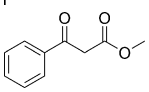	>95; 80	>95; 62	>95; 41	75; 91 >95; 92[d]	36; 94 >95; 95[d]
6[e]	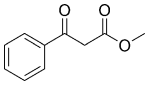	>95; 92	>95; 91	>95; 91	>95; 91	80; 91

[a] Reaction conditions: Substrate (0.2 mmol) in solvent (CH_2Cl_2/MeOH = 2:1, v/v; 1.5 mL), substrate/catalyst = 500 (entries 1) and 200 (entries 2–6), 50 atm H_2, 60 °C, 24 h. [b] Based on ^{1}H NMR spectroscopic analysis of the crude product. [c] Determined by HPLC with chiral OD-H (**2a** and **2e**) and OB-H (**2b–d**) columns. [d] 5 mol% TsOH·H_2O was added as additive. [e] Dendritic [Ru(**G$_n$-DenBINAP**)] catalysts were used, which were generated in situ from [$RuCl_2$(*p*-cymene)] and **G$_n$-DenBINAP** (n = 0–4).[8b,e]

(*ee*) of 66 and 44%, respectively, which were lower than that obtained from the parent **MeO-BINAP** catalyst. In contrast, when the higher-generation **G_2-BINAP** and **G_3-BINAP** catalysts were used, the enantioselectivity increased gradually, giving β-hydroxyl acid ester with 92 and 97% *ee*, respectively, which were obviously superior to the parent catalyst. To further investigate the synthetic utility of our dendritic catalyst, hydrogenation of some β-aryl β-ketoester substrates were studied. As shown in Table 1 (entries 2–5), quite a similar tendency of variation in enantioselectivity among different generation dendritic catalysts was observed. Excellent enantioselectivities (up to 97% *ee*) for all four substrates were obtained when using higher-generation catalysts. Notably, low conversions were observed in some cases, suggesting that the reactivity decreased with increasing generation of catalyst. This was probably due to the steric effect of the more bulky dendritic wedges, and similar phenomena were observed for other core-functionalized dendrimer catalysts. It is worth mentioning that full conversions and the same enantioselectivityies could be achieved in the presence of 5 mol% TsOH (entry 5, Table 1).[25] For comparison, ruthenium complexes of **G_n-DenBINAP** ligands, which contain dendritic wedges at the 5,5′-positions of the binaphthyl backbone instead of on the P atoms were employed in this reaction (Scheme 2). It was found that the generation number (i.e., the size of the dendritic wedges) did not influence the enantioselectivity at all (entry 6, Table 1). Thus, these results suggested that the sterically demanding dendritic wedges attached on the P atoms could fine-tune the chiral array of the four phenyl rings around the metal center, which are consistent with the rationale of designing such chiral dendritic catalysts.

Table 2. Asymmetric hydrogenation of α-ketoesters with dendritic [Ru(BINAP)].[a]

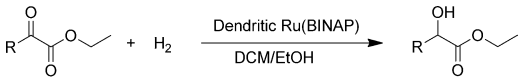

3a-k 4a-k

Entry	Ligand	Substrate (R)	Conv. [%][b]	*ee* [%][c]
1	**MeO-BINAP**	C_6H_5 (**3a**)	>95	84 (96)[d]
2	**G_0-BINAP**	C_6H_5 (**3a**)	>95	70 (96)[d]
3	**G_1-BINAP**	C_6H_5 (**3a**)	>95	59 (96)[d]
4	**G_2-BINAP**	C_6H_5 (**3a**)	>95	93 (94)[d]
5	**G_3-BINAP**	C_6H_5 (**3a**)	>95	95 (94)[d]
6	**G_2-BINAP**	C_6H_5 (**3a**)	>95	93
7	**G_2-BINAP**	C_6H_5 (**3a**)	>95	91
8	**G_2-BINAP**	4-Me-C_6H_4 (**3b**)	>95	91
9	**G_2-BINAP**	4-F-C_6H_4 (**3c**)	>95	94
10	**G_2-BINAP**	4-Cl-C_6H_4 (**3d**)	>95	94
11	**G_2-BINAP**	3-MeO-C_6H_4 (**3e**)	>95	94
12	**G_2-BINAP**	3-Cl-C_6H_4 (**3f**)	>95	92
13	**G_2-BINAP**	2-MeO-C_6H_4 (**3g**)	>95	86
14	**G_2-BINAP**	2-Cl-C_6H_4 (**3h**)	>95	83
15	**G_2-BINAP**	3,5-diMe-C_6H_3 (**3i**)	>95	94
16	**G_2-BINAP**	2-naphthyl (**3j**)	>95	93
17	**G_2-BINAP**	phenethyl (**3k**)	>95	83

[a] Reaction conditions: Substrate (1.0 mmol) in solvent (CH_2Cl_2/EtOH = 2:1, 3.0 mL v/v), substrate/catalyst = 1000 (except for entries 6 and 7, substrate/catalyst = 5000 and 10000), 15 mol% $FeCl_2$, 50 atm H_2, 60 °C, 24 h. [b] Based on ^{1}H NMR spectroscopic analysis of the crude product. [c] Determined by HPLC with chiral AD-H (**4a–h** and **4j**), OD-H (**4i** and **4k**) columns. [d] Data in brackets were obtained with 0.2 mol% dendritic [Ru(**G_n-DenBINAP**)] (n = 0–4) catalysts under otherwise identical conditions.

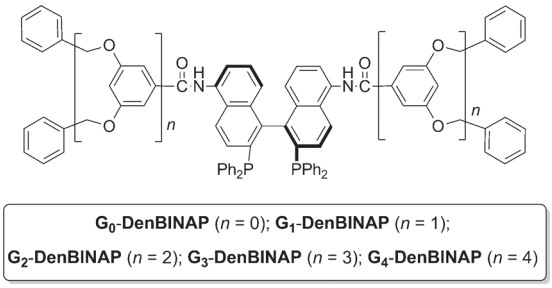

G_0-DenBINAP (n = 0); **G_1-DenBINAP** (n = 1); **G_2-DenBINAP** (n = 2); **G_3-DenBINAP** (n = 3); **G_4-DenBINAP** (n = 4)

Scheme 2. Molecular structures of chiral dendritic **G_n-DenBINAP** ligands.

Asymmetric hydrogenation of α-ketoesters

Optically pure α-hydroxyl esters and their derivatives are important building blocks for the synthesis of pharmacologically active and naturally occurring compounds.[26] In contrast to the great progress made in the asymmetric hydrogenation of β-ketoesters, the success in the homogeneous asymmetric hydrogenation of α-ketoesters, particularly, α-aryl ketoesters has been quite limited.[14d,25a,27] Thus, the development of new effective catalytic systems is still of great importance. On the basis of the excellent performance of our dendritic ruthenium catalysts in the hydrogenation of β-ketoesters, we then applied our catalytic system in the asymmetric hydrogenation of α-ketoesters, and the results are summarized in Table 2. It was found that hydrogenation reactions catalyzed by these ruthenium catalysts proceeded smoothly in the presence of 15 mol% $FeCl_2$.[28] Notably, a remarkable dendrimer effect was also observed in such transformations, which is similar to that observed in the hydrogenation of β-ketoesters (entries 1–5, Table 2). The highest *ee* value of 95% was obtained with the third-generation catalyst. It is worth mentioning that with even the use of 0.01 mol% **G_2-BINAP** catalyst, full conversion with 91% *ee* was obtained (entry 7, Table 2). In addition, various α-aryl ketoesters bearing electron-donating- or electron-withdrawing substituents were successfully hydrogenated by using 0.1 mol% **G_2**-BINAP catalyst, providing chiral α-hydroxyl esters in full conversions with quite good enantioselectivities (entries 8–16, Table 2). Only the substrates bearing substituents at the *ortho* position of the phenyl ring gave relatively low enantioselectivities (entries 13 and 14, Table 2). Substrate α-alkyl ketoester **3k** could also be hydrogenated to give the reduced product with good enantioselectivity (entry 17, Table 2). Notably, ruthenium complexes of **G_n-DenBINAP** ligands were also effective for such transformation, but the generation number did not obviously influence the enantioselectivity (entries 1–5, Table 2).

Asymmetric hydrogenation of α-ketoamides

Optically active α-hydroxyl amides are important chiral building blocks for the synthesis of biologically active compounds and chiral ligands for enantioselective addition reaction.[26a,29] Accordingly, many efforts have been devoted to their preparation through asymmetric synthesis. Among the various methods for synthesizing chiral α-hydroxyl amides, including enantioselective Passerini-type reaction,[30a] ring opening of chiral α,β-epoxy amides,[30b] and asymmetric oxidation of racemic α-hydroxy amides,[30c] the asymmetric hydrogenation of the corresponding prochiral α-ketoamides represents one of the most direct and efficient approaches for attaining such chiral compounds. However, in sharp contrast to the β-ketoester and α-ketoester substrates, asymmetric hydrogenation of α-ketoamides has been less studied. Only a few examples were reported on the asymmetric hydrogenation of α-ketoamides, which still suffered from low efficiency and limited substrate scope.[31] Encouraged by the excellent performance of our dendritic catalysts in the asymmetric hydrogenation of both β-ketoester and α-ketoester substrates, we further applied our catalytic system to the asymmetric hydrogenation of these less studied α-ketoamides.

Under the optimized conditions for the asymmetric hydrogenation of α-ketoester substrates, a wide range of α-ketoamides were smoothly hydrogenated in the presence of 1.0 mol% ruthenium catalyst. As shown in Table 3, the dendritic wedges played an important role in achieving high enantioselectivity, the same phenomena was observed in the hydrogenation of β-ketoesters and α-ketoesters (entries 1–5, Table 3). Excellent enantioselectivities were achieved by using high-generation catalysts, which are much better than those obtained from the small molecular catalysts. Notably, the enantioselectivity was found to be sensitive to the substituent number on the N atom. All α-alkyl ketoamides bearing two substituents gave very good enantioselectivities by using the second-generation catalyst (entries 4–11, Table 3). Hydrogenation of α-alkyl Weinreb amide **5g** also proceeded smoothly to give the product with 94% *ee*. To the best of our knowledge, these represent the highest enantioselectivities for the asymmetric hydrogenation of α-alkyl ketoamides. In addition, several α-aryl ketoamides were also tested, and the substituents on the N atom had an obvious influence on the reactivity (entries 14–17, Table 3). Substrate **5j** bearing methyl and phenyl groups on the N atom could not be reduced at all (entry 14, Table 3). Full conversions and moderate enantioselectivities for other substrates bearing only one substituent were observed (entries 15–17, Table 3). For comparison, ruthenium complexes of **G_n-DenBINAP** ligands were also applied for this reaction and exhibited excellent enantioselectivities (entries 1–5, Table 3). However, the generation number did not obviously influence the enantioselectivity. Finally, the absolute configuration of the α-hydroxyl amide product **6a** was determined to be *R* based on single-crystal X-ray analysis (for details, see the Supporting Information).[32] Thus, the hydride was supposed to attack the *si*-face of the α-ketoamides, which was the same as that for α-ketoesters.

Table 3. Asymmetric hydrogenation of α-ketoamides with dendritic [Ru(BINAP)].[a]

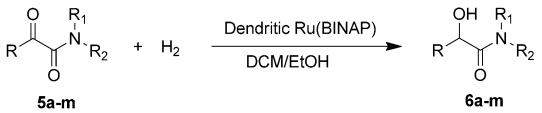

5a-m **6a-m**

Entry	Ligand	Substrate ($R/R^1/R^2$)	Conv. [%][b]	*ee* [%][c]
1	**MeO-BINAP**	Et/Me/Ph (**5a**)	>95	85 (98)[d]
2	**G_0-BINAP**	Et/Me/Ph (**5a**)	>95	70 (98)[d]
3	**G_1-BINAP**	Et/Me/Ph (**5a**)	>95	52 (98)[d]
4	**G_2-BINAP**	Et/Me/Ph (**5a**)	>95	95 (97)[d]
5	**G_3-BINAP**	Et/Me/Ph (**5a**)	>95	98 (96)[d]
6	**G_2-BINAP**	Me/Me/Ph (**5b**)	>95	89
7	**G_2-BINAP**	$PhCH_2CH_2$/Me/Ph (**5c**)	>95	95
8	**G_2-BINAP**	$PhCH_2CH_2$/Me/Me (**5d**)	>95	94
9	**G_2-BINAP**	$PhCH_2CH_2$/Et/Et (**5e**)	>95	95
10	**G_2-BINAP**	$PhCH_2CH_2$/-$(CH_2)_4$- (**5f**)	>95	93
11	**G_2-BINAP**	$PhCH_2CH_2$/OMe/Me (**5g**)	>95	94
12	**G_2-BINAP**	$PhCH_2CH_2$/H/*i*Pr (**5h**)	>95	85
13	**G_2-BINAP**	$PhCH_2CH_2$/H/Ph (**5i**)	>95	80
14	**G_2-BINAP**	Ph/Me/Ph (**5j**)	<5	–
15	**G_2-BINAP**	Ph/H/Ph (**5k**)	>95	73
16	**G_2-BINAP**	Ph/H/Bn (**5l**)	>95	73
17	**G_2-BINAP**	Ph/H/*n*-Pr (**5m**)	>95	78

[a] Reaction conditions: Substrate (0.1 mmol) solvent (CH_2Cl_2/EtOH = 2:1, v/v, 1.5 mL), substrate/catalyst = 100 (mol/mol), 15 mol% $FeCl_2$, 50 atm H_2, 60 °C, 24 h. [b] Based on ^{1}H NMR spectroscopic analysis of the crude product. [c] Determined by HPLC with chiral OJ-H (**6a–f**), OD-H (**6g**), and AD-H (**6h–m**) columns. [d] Data in brackets were obtained with 1.0 mol% dendritic [Ru(**G_n-DenBINAP**)] (n = 0–4) catalysts under otherwise identical conditions.

Catalyst recycling

As mentioned above, the dendritic catalysts could be easily precipitated quantitatively by adding protonic solvent. The recyclability of the dendritic catalyst was then investigated by using the **G_2-BINAP** catalyst, and the hydrogenation of α-aryl ketoester **1e** was chosen as the standard reaction (Table 4). Upon the completion of the reaction, degassed methanol was

Table 4. Catalyst recycling.[a]

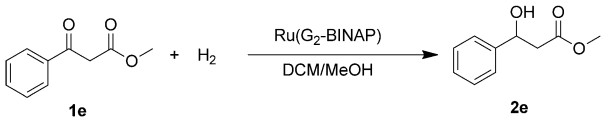

1e **2e**

Run	*t* [h]	Conv. [%]	*ee* [%]
1	24	>95	92
2	24	>95	91
3	40	>95	92
4	40	>95	90
5	40	>95	88
6	40	93	87
7	40	87	88
8	40	76	89

[a] Reaction conditions: Substrate (0.6 mmol) in (CH_2Cl_2/MeOH = 2:1, v/v, 4.5 mL), substrate/catalyst = 200, 5 mol% TsOH, 50 atm H_2, 60 °C.

added to the reaction mixture, and the precipitated catalyst was collected by filtration and used for the next catalytic run. Gratifyingly, the catalyst could be reused at least 7 times with no obvious decrease in enantioselectivity (entries 1–8, Table 4). Notably, the reaction rate decreased slightly, but full conversions were still obtained before run 6 upon prolonging the reaction time. The decrease in reactivity was probably due to the oxidation of catalyst during the recycling process.

Computational study of the tunable dendritic [Ru(BINAP)] complexes

It has been well known that coordination of BINAP ligand to Ru^{II} species makes a conformationally unambiguous seven-membered chelate complex. Its dissymmetric structure determines the chiral array of the four phenyl rings on the P atoms, which form the chiral pocket of the catalyst at which the enantioselective reaction occurs.[18] For the dendritic BINAP ligands, we envision that the increasing steric repulsion between the four larger dendritic wedges with the increase of generation can influence the chiral array of the four phenyl rings, and consequently modulate the catalytic behavior of the core. To further understand this unusual "dendritic effect" observed, theoretical calculations were carried out.

By employing the semi-empirical PM6 method[33] in the Gaussian 09 program,[34] we fully optimized the molecular structures of the four dendritic [Ru(**G_n-BINAP**)] complexes and [Ru(**MeO-BINAP**)]. To confirm that semi-empirical PM6 method is reliable here, we also performed first principle DFT calculations for the smallest complexes from **MeO-BINAP**, the larger congeners of which are too large to be done with DFT calculations. The geometric results of DFT calculations are similar with PM6 results as shown in the Supporting Information (Table S1), which indicates that PM6 is the appropriate method here. The optimized structure of dendritic [Ru(**G_n-BINAP**)] complex with the numbering scheme is schematically shown in Figure 2.

We list several geometric parameters of the optimized structures in Table 5 and Table 6. The results show that the dihedral angle (D1) between the two naphthalene rings of BINAP unit and the P1-Ru-P2 angle are almost unchanged in this series of complexes (Table 5), which were proven to play an important role in achieving high enantioselectivity for other types of tunable chiral biaryl diphosphine ligands.[14a,d,20b] To further explore the effect of bulky dendritic wedges on chiral environment around the metal center, we employed an atom-to-plane distance analysis as used in a previous study.[35] The distances of carbon atoms in the phenyl ring on P2-atom from the plane (labeled by a dotted oval in Figure 2) passing through the Ru atom and perpendicular to the axis (labeled as "Z" in Figure 2), which passes through Ru and meets at right angles with P1-P2 show apparent disparity in the BINAP ligands (Table 6). These distances in **MeO-BINAP**, **G_2-BINAP**, and **G_3-BINAP** systems are larger than the corresponding ones in **G_0-BINAP** and **G_1-BINAP** systems, indicating that the phenyl rings of high-generation ligands and **MeO-BINAP** protrude to the other P-Ru-P in-plane coordination sites to a greater extent as compared with those of low generation ligands. This distance trend, which reflects the difference in steric environments around the metal center, is in agreement with that of enantioselectivity observed in the asymmetric hydrogenation of all three kinds of ketones.

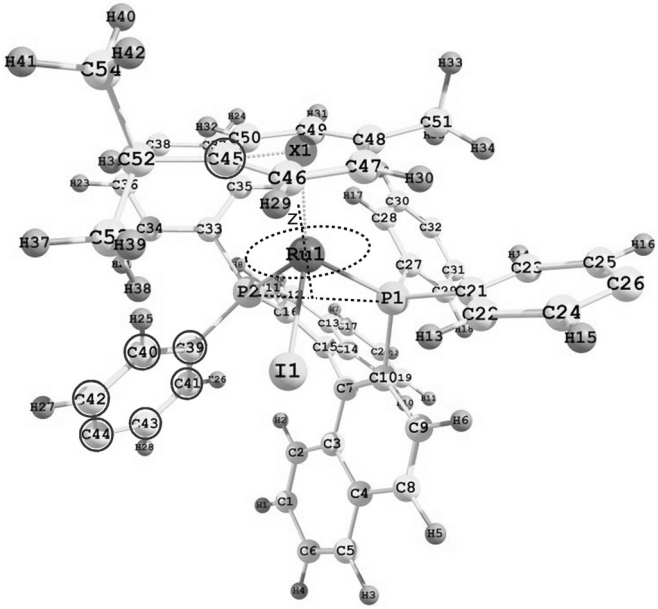

Figure 2. The optimized structure of dendritic [Ru(**G_n-BINAP**)] complex with the dendritic wedges omitted for clarity (X is the center of the *p*-cymene ring, "Z" is the axis passing through Ru and meeting at right angles with P1-P2).

Table 5. Calculated dihedral angles D1 (between the two naphthalene rings of BINAP unit), D2 (between the C45-X-Ru plane and the X-Ru-I plane), and the P1-Ru-P2 angle of [Ru(**MeO-BINAP**)] and [Ru(**G_n-BINAP**)] complexes, all in degrees.[a]

Ligand	MeO-BINAP	G_0-BINAP	G_1-BINAP	G_2-BINAP	G_3-BINAP
D1	76.5	76.9	76.6	76.8	76.2
D2	57.7	51.8	51.7	56.3	55.9
P1-Ru-P2	96.4	96.7	96.3	96.7	96.4

[a] Atomic numberings are shown in Figure 2, X is the center of the *p*-cymene ring.

Table 6. Distances [Å] of carbons in the phenyl rings of [Ru(**G_n-BINAP**)] complexes from the plane passing through the Ru atom and perpendicular to the axis that passes through Ru and meets at right angles with P1-P2.[a]

C atom No.	MeO-BINAP	G_0-BINAP	G_1-BINAP	G_2-BINAP	G_3-BINAP
C39	1.76	1.63	1.64	1.78	1.75
C40	0.66	0.46	0.47	0.68	0.63
C41	3.05	2.88	2.90	3.08	3.04
C42	0.83	0.52	0.54	0.86	0.80
C43	3.25	2.97	2.99	3.29	3.24
C44	2.13	1.78	1.80	2.17	2.11

[a] The atom-numbering scheme of [Ru(**G_n-BINAP**)] complexes is shown in Figure 2.

Considering that the co-ligand *p*-cymene will be replaced by ketone substrates in the hydrogenation process, we further choose this co-ligand as a probe to measure the chiral pocket of these dendritic Ru catalysts. The dihedral angle (D2) between the plane C45-X-Ru (X is the center of the *p*-cymene ring) and the plane X-Ru-I, which represents the rotation of *p*-cymene, is listed in Table 5. Clearly, the dihedral angles of **G_0-BINAP** and **G_1-BINAP** systems are different from those of **MeO-BINAP**, **G_2-BINAP** and **G_3-BINAP** systems. Notably, both the dihedral angle trend and the distance trend discussed above are in accord. All these results suggest that the attachment of bulky dendritic wedges on the four phenyl rings at P atoms will fine-tune the steric environments around the metal center. The increasing steric repulsion interaction between dendritic wedges might be responsible for the different array of the four phenyl rings, and consequently modulate the catalytic behavior of the [Ru(**G_n-BINAP**)] complexes, as shown in Figure 3.

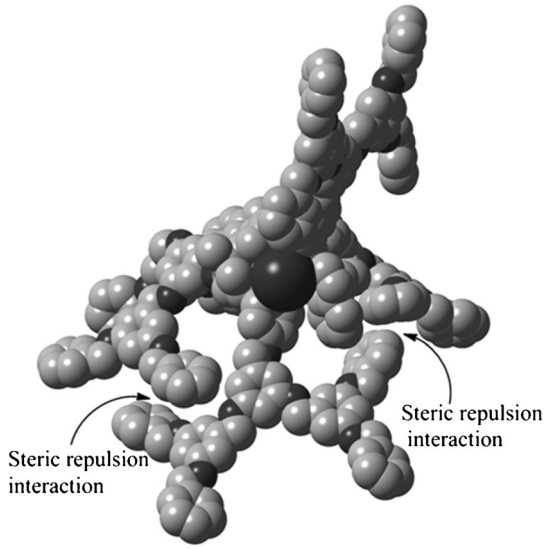

Figure 3. Optimized structure of the [Ru(**G_2-BINAP**)] complex.

For comparison, we also investigate the three parameters described above for similar dendritic [Ru(**G_n-DenBINAP**)] catalysts, in which the dendritic wedges are attached at the 5,5′-positions of binaphthyl backbone of BINAP unit as shown in Scheme 2. The data are summarized in Table 7. Expectedly, both dihedral angles (D1 and D2) and P1-Ru-P2 angles in this series of [Ru(**G_n-DenBINAP**)] complexes do not show apparent variation. These results indicate that the bulky dendritic wedges on the naphthalene rings do not significantly interact with one another, and consequently do not influence the chiral pocket of the catalyst where the hydrogenation reaction occurs, which is consistent with the experiment results.

Table 7. Calculated dihedral angles D1, D2, and BINAP–Ru binding angle (P1-Ru-P2) for the five [Ru(**G_n-DenBINAP**)] molecular structures, all in degrees.[a]

Ligand	G_0-DenBINAP	G_1-DenBINAP	G_2-DenBINAP	G_3-DenBINAP	G_4-DenBINAP
D1	76.6	76.6	76.6	76.5	77.9
D2	51.7	52.4	52.9	52.5	52.1
P1-Ru-P2	96.3	96.3	96.2	96.1	96.1

[a] The three parameters are same as ones described in Table 5.

Conclusion

We have developed a new family of tunable dendritic BINAP ligands by attaching polyaryl ether dendrons onto the four phenyl rings on the P atoms. These dendritic ligands were applied to the ruthenium-catalyzed asymmetric hydrogenation of β-ketoesters, α-ketoesters, as well as the less-studied α-ketoamides. It was found that the size of the dendritic wedges played important roles in catalytic performance. The unusual enantioselectivity profile of **G_3-BINAP** > **G_2-BINAP** > **MeO-BINAP** > **G_0-BINAP** > **G_1-BINAP** was observed in the hydrogenation of all three kinds of substrates. The high-generation catalysts exhibited excellent enantioselectivities, which are superior to those obtained from the small molecular catalysts. On the other hand, the larger dendrons led to decreased reactivity due to the steric effect of the more bulky dendritic wedges. Further molecular modeling indicates that the attachment of bulky dendritic wedges on the four phenyl rings at P atoms can fine-tune the steric environments around the metal center. The increasing steric repulsion interaction between dendritic wedges might be responsible for the different array of the four phenyl rings, and consequently modulate and improve the enantioselectivity. In addition, the second-generation catalyst could be easily recovered by solvent precipitation and reused at least seven times without obvious decrease in enantioselectivity. Since most phosphorus ligands contain "PPh_2" units, this method can be extended to other synthetically useful chiral phosphorus-containing dendritic catalysts. The use of these tunable and recyclable chiral dendritic diphosphines to other asymmetric catalytic reactions is in progress.

Experimental Section

General

All chemicals were obtained from Aldrich, Alfa, or Acros and used as received unless otherwise mentioned. The organic solvents used were dried according to published methods. Unless otherwise noted, all reactions were performed under an atmosphere of dinitrogen employing standard Schlenk techniques. ^{1}H NMR, ^{13}C NMR, and ^{31}P NMR spectra were recorded on Bruker AMX 300 Spectrometer (^{1}H: 300 MHz; ^{13}C: 75 MHz; ^{31}P: 121 MHz) or Bruker AMX-600 spectrometers (^{1}H: 600 MHz; ^{13}C: 150 MHz; ^{31}P: 243 MHz) at 298 K. Chemical shifts are reported in parts per million (ppm) relative to the internal standards, partially deuterated solvents or tetramethylsilane (TMS). Coupling constants (*J*) are denoted in Hz and chemical shifts (δ) in ppm. Multiplicities are denoted as follows: s = singlet, d = doublet, m = multiplet, br = broad. Matrix-assisted laser desorption-ionization (time of flight) mass spectrometry (MALDI-TOF) was performed on a Bruker Biflex III MALDI-TOF spectrometer with α-cyano-4-hydroxylcinnamic acid (CCA) as the matrix. HRMS-FAB spectra were carried out on a Bruker APEX 47E FTMS spectrometer. HRMS-ESI

mass spectra were obtained on a Bruker APEX IV instrument. Elemental analyses were performed on a Carlo–Erba-1106 instrument. The detailed spectroscopic and analytical data of all known and new compounds is provided in the Supporting Information.

General procedure for the synthesis of chiral dendritic diphosphine oxides G_n-BINAPO

A mixture of **OH-BINAPO**, **G_n-Br** (6.0 equiv), K_2CO_3 (6.0 equiv), KI (1.0 equiv), and a catalytic amount of 18-crown-6 in acetone was stirred at 80 °C for 20 h. After being cooled to room temperature, the organic solvent was evaporated under reduced pressure. The residue was further purified by precipitation into methanol and/or by silica column chromatography, giving the desired chiral dendritic **G_n-BINAPO** as an off-white powder.

G_0-BINAPO: Treatment of **OH-BINAPO** (0.15 g, 0.2 mmol) and **G_0-Br** (0.21 g, 1.2 mmol) in acetone as the above procedure to give **G_0-BINAPO** (0.19 g, 70%). ^{1}H NMR (300 MHz, $CDCl_3$): δ = 7.75–7.78 (m, 4H), 7.51–7.58 (m, 4H), 7.30–7.40 (m, 28H), 6.75–6.83 (m, 12H), 5.03 (s, 4H), 4.96 ppm (s, 4H); ^{13}C NMR (75 MHz, $CDCl_3$): δ = 160.9, 136.5, 134.5, 134.3, 133.9, 133.7, 128.7, 128.6, 128.3, 128.1, 128.1, 127.7, 127.6, 127.5, 127.3, 127.1, 125.8, 114.4, 114.2, 69.9 ppm; ^{31}P NMR (121 MHz, $CDCl_3$): δ = 27.3 ppm. MS (MALDI-TOF): *m/z* calcd (%) for $C_{72}H_{56}O_6P_2$: 1080.2 $[M+H]^+$; found: 1079.2.

G_1-BINAPO: Treatment of **OH-BINAPO** (0.15 g, 0.2 mmol) and **G_1-Br** (0.46 g, 1.2 mmol) in acetone as the above procedure giving **G_1-BINAPO** (0.33 g, 85%). ^{1}H NMR (300 MHz, $CDCl_3$): δ = 7.72–7.84 (m, 4H), 7.60–7.67 (m, 4H), 7.25–7.41 (m, 44H), 7.14–7.21 (m, 4H), 6.82–6.94 (m, 6H), 6.56–6.67 (m, 18H), 4.94–5.03 ppm (m, 24H); ^{13}C NMR (75 MHz, $CDCl_3$): δ = 161.1, 161.0, 160.3, 160.3, 139.1, 139.0, 136.9, 136.8, 134.6, 134.4, 134.1, 133.8, 128.7, 128.7, 128.2, 128.1, 127.7, 127.4, 114.6, 106.5, 101.8, 101.7, 70.3, 70.2, 69.9 ppm; ^{31}P NMR (121 MHz, $CDCl_3$): δ = 26.8 ppm. MS (MALDI-TOF): *m/z* calcd for $C_{128}H_{104}O_{14}P_2$: 1929.1: $[M+H]^+$; found:1928.0.

G_2-BINAPO: Treatment of **OH-BINAPO** (0.15 g, 0.2 mmol) and **G_2-Br** (0.97 g, 1.2 mmol) in acetone as the above procedure giving **G_2-BINAPO** (0.65 g, 90%). ^{1}H NMR (300 MHz, $CDCl_3$): δ = 7.62–7.68 (m, 4H), 7.43–7.50 (m, 4H), 7.07–7.34 (m, 90H), 6.64–6.70 (m, 10H), 6.43–6.55 (m, 36H), 4.75–4.86 ppm (m, 56H); ^{13}C NMR (75 MHz, $CDCl_3$): δ = 160.9, 160.3, 160.2, 160.1, 160.0, 144.2, 143.0, 139.5, 139.3, 139.2, 139.1, 139.0, 136.9, 136.8, 134.6, 133.9, 133.8, 133.6, 130.1, 128.6, 128.6, 128.3, 128.1, 128.0, 127.8, 127.6, 127.2, 125.9, 114.5, 114.3, 106.5, 105.6, 101.7, 101.2, 70.1, 70.1, 70.0, 69.8 ppm; ^{31}P NMR (121 MHz, $CDCl_3$): δ = 28.3 ppm; MS (MALDI-TOF): *m/z* calcd for $C_{240}H_{200}O_{30}P_2$: 3627.1 $[M+H]^+$; found: 3626.1.

G_3-BINAPO: Treatment of **OH-BINAPO** (0.08 g, 0.1 mmol) and **G_3-Br** (0.99 g, 0.6 mmol) in acetone as the above procedure giving **G_3-BINAPO** (0.60 g, 86%). ^{1}H NMR (300 MHz, $CDCl_3$): δ = 7.70–7.74 (m, 4H), 7.42–7.56 (m, 4H), 7.15–7.37 (m, 170H), 6.46–6.86 (m, 94H), 4.65–5.00 ppm (m, 120H); ^{13}C NMR (75 MHz, $CDCl_3$): δ = 160.2, 160.1, 160.1, 160.0, 139.3, 139.2, 139.0, 136.8, 128.6, 128.6, 128.0, 128.0, 127.6, 114.4, 106.4, 101.6, 70.1, 70.0, 69.9 ppm; ^{31}P NMR (121 MHz, $CDCl_3$): δ = 27.7 ppm. MS (MALDI-TOF): *m/z* calcd for $C_{464}H_{392}O_{62}P_2$: 7023.0 $[M+H]^+$; found: 7025.

General procedure for the synthesis of chiral dendritic diphosphine ligands G_n-BINAP

Trichlorosilane (10 equiv) was added carefully at 0 °C to a mixture of **G_n-BINAPO** and N(*n*-Bu)$_3$ (20 equiv) in degassed toluene under nitrogen atmosphere. The mixture was then stirred at 120 °C for 24 h. After being cooled to room temperature, degassed NaOH solution (4 M, 20 equiv) was added carefully. Then, the mixture was stirred at 80 °C until the organic layer became clear. The organic layer was separated at room temperature, washed with water, dried over Na_2SO_4, and concentrated under reduced pressure. The residue was further purified by precipitation into methanol and/or by silica column chromatography, giving the desired chiral dendritic **G_n-BINAP** ligands as an off-white powder.

G_0-BINAP: Treatment of **G_0-BINAPO** (1.08 g, 1 mmol) with trichlorosilane (1 mL, 10 mmol) in toluene as the above procedure giving **G_0-BINAP** (0.77 g, 80%). ^{1}H NMR (300 MHz, $CDCl_3$): δ = 7.86–7.89 (m, 2H), 7.80–7.82 (m, 2H), 7.29–7.46 (m, 24H), 6.85–7.06 (m, 10H), 6.69–6.79 (m, 10H), 4.94–4.98 ppm (m, 8H); ^{13}C NMR (75 MHz, $CDCl_3$): δ = 144.7, 144.4, 137.0, 137.0, 136.3, 136.0, 135.9, 135.7, 135.6, 134.5, 134.3, 134.2, 133.5, 133.4, 133.4, 133.2, 130.2, 129.3, 129.2, 129.1, 129.0, 128.9, 128.6, 128.6, 128.4, 128.1, 128.0, 127.7, 127.6, 127.5, 127.1, 127.0, 126.4, 125.8, 114.7, 114.7, 113.3, 70.6, 69.9, 69.8 ppm; ^{31}P NMR (121 MHz, $CDCl_3$): δ = −20.0 ppm; MS (MALDI-TOF): *m/z* calcd for $C_{72}H_{56}O_4P_2$: 1048.2 $[M+H]^+$; found: 1045.5; elemental analysis calcd (%) for $[C_{72}H_{56}O_4P_2]$: C, 82.58; H, 5.39; found: C, 82.43; H, 5.68.

G_1-BINAP: Treatment of **G_1-BINAPO** (0.97 g, 0.5 mmol) with trichlorosilane (0.5 mL, 5 mmol) in toluene as the above procedure giving **G_1-BINAP** (0.78 g, 82%). ^{1}H NMR (300 MHz, $CDCl_3$): δ = 7.84–7.87 (m, 2H), 7.77–7.80 (m, 2H), 7.24–7.45 (m, 44H), 6.84–7.02 (m, 10H), 6.52–6.76(m, 22H), 4.86–5.02 ppm (m, 24H); ^{13}C NMR (75 MHz, $CDCl_3$): δ = 160.2, 159.1, 158.6, 1445.0, 144.7, 144.3, 139.5, 136.9, 136.8, 136.5, 135.9, 135.8, 135.6, 134.5, 134.3, 134.2, 133.5, 133.4, 133.2, 130.3, 129.4, 129.4, 129.1, 129.1, 128.7, 128.6, 128.1, 128.1, 127.6, 127.5, 126.4, 125.8, 114.8, 106.4, 101.7, 101.6, 70.2, 70.1, 69.9, 69.8 ppm; ^{31}P NMR (121 MHz, $CDCl_3$): δ = −19.2 ppm. MS (MALDI-TOF): *m/z* calcd for $C_{128}H_{104}O_{12}P_2$: 1897.1 $[M+H]^+$, found: 1896.1; elemental analysis calcd (%) for $[C_{128}H_{104}O_{12}P_2]$: C 81.08; H 5.53; found: C 80.53; H 5.66.

G_2-BINAP: Treatment of **G_2-BINAPO** (1.82 g, 0.5 mmol) with trichlorosilane (0.5 mL, 5 mmol) in toluene as the above procedure giving **G_2-BINAP** (1.49 g, 83%). ^{1}H NMR (300 MHz, $CDCl_3$): δ = 7.83–7.86 (m, 2H), 7.76–7.79 (m, 2H), 7.26–7.39 (m, 84H), 6.89–7.02 (m, 10H), 6.48–6.87 (m, 46H), 4.84–5.02 ppm (m, 56H); ^{13}C NMR (75 MHz, $CDCl_3$): δ = 160.8, 160.1, 160.0, 160.0, 159.0, 159.5, 144.9, 144.7, 144.4, 139.4, 139.2, 139.1, 138.9, 136.7, 136.7, 136.3, 135.8, 135.5, 134.2, 133.3, 133.1, 130.7, 130.6, 130.2, 129.0, 128.5, 127.9, 127.7, 127.5, 127.1, 126.4, 125.8, 114.7, 106.3, 101.5, 69.9 ppm; ^{31}P NMR (121 MHz, $CDCl_3$): δ = −19.2 ppm; MS (MALDI-TOF): *m/z* calcd for $C_{240}H_{200}O_{28}P_2$: 3595.1 $[M+H]^+$; found: 3596.3; elemental analysis calcd (%) for $[C_{240}H_{200}O_{28}P_2]$: C 80.20; H 5.61; found: C 80.15; H 5.67.

G_3-BINAP: Treatment of **G_3-BINAPO** (1.76 g, 0.25 mmol) with trichlorosilane (0.25 mL, 2.5 mmol) in toluene as the above procedure giving **G_3-BINAP** (1.31 g, 75%). ^{1}H NMR (300 MHz, $CDCl_3$): δ = 7.80–7.82 (m, 2H), 7.74–7.77 (m, 2H), 7.23–7.38 (m, 164H), 6.77–7.05 (m, 12H), 6.44–6.68(m, 92H), 4.75–5.01 ppm (m, 120H); ^{13}C NMR (75 MHz, $CDCl_3$): δ = 160.2, 160.2, 159.2, 158.6, 158.5, 143.7, 139.31, 137.2, 136.9, 136.5, 136.2, 135.8, 134.3, 133.3, 130.4, 128.7, 128.3, 128.1, 127.6, 126.5, 125.9, 114.7, 106.5, 105.8, 101.7, 70.2, 70.1 ppm; ^{31}P NMR (121 MHz, $CDCl_3$): δ = −20.1 ppm. MS (MALDI-TOF): *m/z* calcd for $C_{464}H_{392}O_{60}P_2$: 7029.1 $[M+K]^+$; found: 7025; elemental analysis calcd (%) for $[C_{464}H_{392}O_{60}P_2]$: C 79.73; H 5.65; found: C 79.87; H 5.69.

General procedure for asymmetric hydrogenation and catalyst recycling

In situ catalyst preparation: A 25 mL flask was charged with **G_n-BINAP** (0.11 mmol), $[RuI_2(cymene)]_2$ (0.05 mmol) and degassed sol-

vent (CH_2Cl_2/EtOH = 2:1, v/v, 6 mL). The mixture was stirred at 50 °C for 2 h under nitrogen atmosphere. After cooling to room temperature, the solvent was evaporated under reduced pressure. A brown powder was obtained that was used directly in the catalytic asymmetric hydrogenation without further purification. All in situ-generated ruthenium catalysts were characterized by using ^{31}P NMR spectroscopy.

Asymmetric hydrogenation and catalyst recycling: A 10 mL glass-lined stainless steel reactor with a magnetic stirring bar was charged with ketoester substrate, the above prepared catalyst [Ru(**G_n-BINAP**)], additive if necessary and suitable solvent. The autoclave was closed and was pressurized with H_2 to 50 atm. The mixture was stirred at 60 °C for 24 h. After carefully venting of hydrogen, excess cold methanol was added to the reaction mixture to precipitate the dendritic catalyst. The recovered catalyst was then reused in the next catalytic cycle. The organic layer was used to determine the conversion and enantioselectivity of the reduced product, which were obtained by GC or HPLC analysis with a chiral column.

Acknowledgements

The authors thank the National Natural Science Foundation of China (No. 21232008, 21290194, 21221002), the National Basic Research Program of China (973 program, No. 2010CB833300), and ICCAS (Institute of Chemistry), Chinese Academy of Sciences for financial support.

Keywords: asymmetric catalysis · dendrimers · hydrogenation · ligands · ruthenium

[1] J. M. J. Fréchet, D. A. Tomalia, *Dendrimers and Other Dendritic Polymers*, Wiley, Chichester, **2002**.

[2] For representative reviews, see: a) G. E. Oosterom, J. N. H. Reek, P. C. J. Kamer, P. W. N. M. van Leeuwen, *Angew. Chem.* **2001**, *113*, 1878 – 1901; *Angew. Chem. Int. Ed.* **2001**, *40*, 1828 – 1849; b) D. Astruc, F. Chardac, *Chem. Rev.* **2001**, *101*, 2991 – 3023; c) R. van Heerbeek, P. C. J. Kamer, P. W. N. M. van Leeuwen, J. N. H. Reek, *Chem. Rev.* **2002**, *102*, 3717 – 3756.

[3] Q. H. Fan, K. L. Ding, *Top. Organomet. Chem.* **2011**, *36*, 207 – 246.

[4] J. W. J. Knapen, A. W. van der Made, J. C. de Wilde, P. W. N. M. van Leeuwen, P. Wijkens, D. M. Grove, G. van Koten, *Nature* **1994**, *372*, 659 – 663.

[5] For selected recent reviews, see: a) D. Wang, D. Astruc, *Coord. Chem. Rev.* **2013**, *257*, 2317 – 2334; b) Z. W. Li, J. S. Li, *Curr. Org. Chem.* **2013**, *17*, 1334 – 1349; c) A. M. Caminade, A. Ouali, M. Keller, J. P. Majoral, *Chem. Soc. Rev.* **2012**, *41*, 4113 – 4125.

[6] For reviews on chiral dendrimer catalysts, see: a) J. K. Kassube, L. H. Gade, *Top. Organomet. Chem.* **2006**, *20*, 61 – 96; b) A. M. Caminade, P. Servin, R. Laurent, J. P. Majoral, *Chem. Soc. Rev.* **2008**, *37*, 56 – 67; c) B. D. Ma, Q. H. Fan, *Sci. Sin. Chim.* **2010**, *40*, 827 – 836.

[7] a) B. Helms, J. M. J. Fréchet, *Adv. Synth. Catal.* **2006**, *348*, 1125 – 1148; b) L. J. Twyman, A. S. H. King, I. K. Martin, *Chem. Soc. Rev.* **2002**, *31*, 69 – 82; c) H. F. Chow, C. F. Leung, G. X. Wang, Y. Y. Yang, *C. R. Chim.* **2003**, *6*, 735 – 745.

[8] For selected examples of chiral dendrimer catalysts with positive dendrimer effect, see: a) R. Breinbauer, E. N. Jacobsen, *Angew. Chem.* **2000**, *112*, 3750 – 3753; *Angew. Chem. Int. Ed.* **2000**, *39*, 3604 – 3607; b) Q. H. Fan, Y. M. Chen, X. M. Chen, D. Z. Jiang, F. Xi, A. S. C. Chan, *Chem. Commun.* **2000**, 789 – 790; c) Y. Ribourdouille, G. D. Engel, M. Richard-Plouet, L. H. Gade, *Chem. Commun.* **2003**, 1228 – 1229; d) A. Gissibl, C. Padié, M. Hager, F. Jaroschik, R. Rasappan, E. Cuevas-Yañez, C. O. Turrin, A. M. Caminade, J. P. Majoral, O. Reiser, *Org. Lett.* **2007**, *9*, 2895 – 2898; e) Z. J. Wang, G. J. Deng, Y. Li, Y. M. He, W. J. Tang, Q. H. Fan, *Org. Lett.* **2007**, *9*, 1243 – 1246; f) F. Zhang, Y. Li, Z. W. Li, Y. M. He, S. F. Zhu, Q. H. Fan, Q. L. Zhou, *Chem. Commun.* **2008**, 6048 – 6050; g) L. Garcia, A. Roglans, R. Laurent, J. P. Majoral, A. Pla-Quintana, A. M. Caminade, *Chem. Commun.* **2012**, *48*, 9248 – 9250; h) J. Liu, Y. Feng, B. D. Ma, Y. M. He, Q. H. Fan, *Eur. J. Org. Chem.* **2012**, 6737 – 6744; i) B. D. Ma, G. J. Deng, J. Liu, Y. M. He, Q. H. Fan, *Acta Chim. Sin.* **2013**, *71*, 528 – 534; j) B. D. Ma, Z. Y. Ding, J. Liu, Y. M. He, Q. H. Fan, *Chem. Asian J.* **2013**, *8*, 1101 – 1104.

[9] R. Noyori, *Angew. Chem.* **2002**, *114*, 2108 – 2123; *Angew. Chem. Int. Ed.* **2002**, *41*, 2008 – 2022.

[10] To the best of our knowledge, only four examples reported a remarkable positive dendrimer effect on the enantioselectivity, see references [8c, d, f, g].

[11] a) Q. H. Fan, Y. M. Li, A. S. C. Chan, *Chem. Rev.* **2002**, *102*, 3385 – 3466; b) Y. Y. Huang, Y. M. He, H. F. Zhou, L. Wu, B. L. Li, Q. H. Fan, *J. Org. Chem.* **2006**, *71*, 2874 – 2877; c) L. Wu, Y. M. He, Q. H. Fan, *Adv. Synth. Catal.* **2011**, *353*, 2915 – 2919; d) Z. Y. Ding, T. L. Wang, Y. M. He, F. Chen, H. F. Zhou, Q. H. Fan, Q. X. Guo, A. S. C. Chan, *Adv. Synth. Catal.* **2013**, *355*, 3727 – 3735.

[12] a) R. Noyori, *Asymmetric Catalysis in Organic Synthesis*, Wiley, New York, **1994**; b) W. Tang, X. Zhang, *Chem. Rev.* **2003**, *103*, 3029 – 3069; c) J. H. Xie, Q. L. Zhou, *Acta Chim. Sin.* **2012**, *70*, 1427 – 1438.

[13] W. S. Knowles, *Angew. Chem.* **2002**, *114*, 2096 – 2107; *Angew. Chem. Int. Ed.* **2002**, *41*, 1998 – 2007.

[14] For selected examples, see: a) Z. G. Zhang, H. Qian, J. Longmire, X. M. Zhang, *J. Org. Chem.* **2000**, *65*, 6223 – 6226; b) J. H. Xie, L. X. Wang, Y. Fu, S. F. Zhu, B. M. Fan, H. F. Duan, Q. L. Zhou, *J. Am. Chem. Soc.* **2003**, *125*, 4404 – 4405; c) A. Hu, H. L. Ngo, W. B. Lin, *Angew. Chem.* **2004**, *116*, 2555 – 2558; *Angew. Chem. Int. Ed.* **2004**, *43*, 2501 – 2504; d) L. Q. Qiu, F. Y. Kwong, J. Wu, W. H. Lam, S. Chan, W. Y. Yu, Y. M. Li, R. W. Guo, Z. Y. Zhou, A. S. C. Chan, *J. Am. Chem. Soc.* **2006**, *128*, 5955 – 5965.

[15] For selected recent reviews, see: a) Z. Wang, G. Chen, K. L. Ding, *Chem. Rev.* **2009**, *109*, 322 – 359; b) A. F. Trindade, P. M. P. Gois, C. A. M. Afonso, *Chem. Rev.* **2009**, *109*, 418 – 514; c) M. Y. Yoon, R. Srirambalaji, K. Kim, *Chem. Rev.* **2012**, *112*, 1196 – 1231.

[16] Chiral dendrimer ligands bearing an achiral diphosphine core and chiral dendritic wedges attached to the four phenyl rings at the P atoms was first reported by Brunner, see: H. Brunner, *J. Organomet. Chem.* **1995**, *500*, 39 – 46.

[17] For dendrimer ligands bearing an achiral diphosphine core and achiral dendritic wedges attached to the four phenyl rings at the P atoms, see: G. E. Oosterom, R. J. van Haaren, J. N. H. Reek, P. C. J. Kamer, P. W. N. M. van Leeuwen, *Chem. Commun.* **1999**, 1119 – 1120.

[18] R. Noyori, H. Takaya, *Acc. Chem. Res.* **1990**, *23*, 345 – 350.

[19] C. J. Hawker, J. M. J. Fréchet, *J. Am. Chem. Soc.* **1990**, *112*, 7638 – 7647.

[20] a) M. Jahjah, M. Alame, S. Pellet-Rostaing, M. Lemaire, *Tetrahedron: Asymmetry* **2007**, *18*, 2305 – 2312; b) G. J. Deng, G. R. Li, L. Y. Zhu, H. F. Zhou, Y. M. He, Q. H. Fan, Z. G. Shuai, *J. Mol. Catal. A* **2006**, *244*, 118 – 123.

[21] M. G. Vinogradov, E. V. Starodubtseva, O. V. Turova, *Russ. Chem. Rev.* **2008**, *77*, 725 – 737.

[22] a) A. Girard, C. Greek, D. Ferroud, J. P. Genet, *Tetrahedron Lett.* **1996**, *37*, 7967 – 7970; b) D. D. Wirth, M. S. Miller, S. K. Boini, T. M. Koenig, *Org. Process Res. Dev.* **2000**, *4*, 513 – 519; c) K. J. Hodgetts, *Tetrahedron Lett.* **2001**, *42*, 3763 – 3766; d) I. S. Ali, A. Sudalai, *Tetrahedron Lett.* **2002**, *43*, 5435 – 5436.

[23] For selected examples, see: a) Y. G. Zhou, W. J. Tang, W. B. Wang, W. G. Li, X. M. Zhang, *J. Am. Chem. Soc.* **2002**, *124*, 4952 – 4953; b) X. B. Wan, Y. H. Sun, Y. F. Luo, D. Li, Z. G. Zhang, *J. Org. Chem.* **2005**, *70*, 1070 – 1072; c) X. F. Sun, W. Li, G. H. Hou, L. Zhou, X. M. Zhang, *Adv. Synth. Catal.* **2009**, *351*, 2553 – 2557; d) J. H. Xie, X. Y. Liu, X. H. Yang, J. B. Xie, L. X. Wang, Q. L. Zhou, *Angew. Chem.* **2012**, *124*, 205 – 207; *Angew. Chem. Int. Ed.* **2012**, *51*, 201 – 203.

[24] R. Noyori, T. Ohkuma, M. Kitamura, H. Takaya, N. Sayo, H. Kumobayashi, S. Akutagawa, *J. Am. Chem. Soc.* **1987**, *109*, 5856 – 5858.

[25] a) K. Mashima, K. Kusano, N. Sato, Y. Matsumura, K. Nozaki, H. Kumobayashi, N. Sayo, Y. Hori, T. Ishizaki, S. Akutagawa, H. Takaya, *J. Org. Chem.* **1994**, *59*, 3064 – 3076; b) Q. H. Fan, C. H. Yeung, A. S. C. Chan, *Tetrahedron: Asymmetry* **1997**, *8*, 4041 – 4045.

[26] a) *α-Hydroxy Acids in Enantioselective Synthesis* (Eds.: G. M. Coppola, H. F. Schuster), Wiley-VCH, Weinheim, **1997**; b) K. Kinbara, *Synlett* **2005**, 732 – 743.

[27] For selected examples, see: a) X. F. Sun, L. Zhou, W. Li, X. M. Zhang, *J. Org. Chem.* **2008**, *73*, 1143 – 1146; b) Q. H. Meng, Y. H. Sun, V. Ratovelomanana-Vidal, J. P. Genet, Z. G. Zhang, *J. Org. Chem.* **2008**, *73*, 3842 – 3847; c) N. W. Boaz, E. B. Mackenzie, S. D. Debenham, S. E. Large, J. A., Jr. Ponasik, *J. Org. Chem.* **2005**, *70*, 1872 – 1880.

[28] Zhang and co-workers reported that Lewis acids as an additive like $[CeCl_3]\cdot 7H_2O$ could dramatically improved enantioselectivity in the Ru-catalyzed asymmetric hydrogenation of aromatic α-ketoesters, see reference [27b].

[29] a) C. Spry, K. Kirk, K. J. Saliba, *FEMS Microbiol. Rev.* **2008**, *32*, 56 – 106; b) G. Blay, I. Fernández, A. Marco-Aleixandre, J. R. Pedro, *J. Org. Chem.* **2006**, *71*, 6674 – 6677; c) S. Stella, A. Chadha, *Catal. Today* **2012**, *198*, 345 – 352; d) M. W. Leighty, B. Shen, J. N. Johnston, *J. Am. Chem. Soc.* **2012**, *134*, 15233 – 15236.

[30] a) S. E. Denmark, Y. Fan, *J. Am. Chem. Soc.* **2003**, *125*, 7825 – 7827; b) H. Kakei, T. Nemoto, T. Ohshima, M. Shibasaki, *Angew. Chem.* **2004**, *116*, 321 – 324; *Angew. Chem. Int. Ed.* **2004**, *43*, 317 – 320; c) S. S. Weng, M. W. Shen, J. Q. Kao, Y. S. Munot, C. T. Chen, *Proc. Natl. Acad. Sci. USA* **2006**, *103*, 3522 – 3527.

[31] a) T. Chiba, A. Miyashita, H. Nohira, H. Takaya, *Tetrahedron Lett.* **1993**, *34*, 2351 – 2354; b) J. F. Carpentier, A. Mortreux, *Tetrahedron: Asymmetry* **1997**, *8*, 1083 – 1099; c) M. M. Zhao, W. F. Li, X. Ma, W. Z. Fan, X. M. Tao, X. M. Li, X. M. Xie, Z. G. Zhang, *Sci. China Chem.* **2013**, *56*, 342 – 348.

[32] CCDC-987977 (**6a′**) contains the supplementary crystallographic data for this paper. These data can be obtained free of charge from The Cambridge Crystallographic Data Centre via www.ccdc.cam.ac.uk/data_request/cif.

[33] J. J. P. Stewart, *J. Mol. Model.* **2007**, *13*, 1173 – 1213.

[34] Gaussian 09, Revision C.01, M. J. Frisch, G. W. Trucks, H. B. Schlegel, G. E. Scuseria, M. A. Robb, J. R. Cheeseman, G. Scalmani, V. Barone, B. Mennucci, G. A. Petersson, H. Nakatsuji, M. Caricato, X. Li, H. P. Hratchian, A. F. Izmaylov, J. Bloino, G. Zheng, J. L. Sonnenberg, M. Hada, M. Ehara, K. Toyota, R. Fukuda, J. Hasegawa, M. Ishida, T. Nakajima, Y. Honda, O. Kitao, H. Nakai, T. Vreven, J. A. Montgomery, Jr., J. E. Peralta, F. Ogliaro, M. Bearpark, J. J. Heyd, E. Brothers, K. N. Kudin, V. N. Staroverov, R. Kobayashi, J. Normand, K. Raghavachari, A. Rendell, J. C. Burant, S. S. Iyengar, J. Tomasi, M. Cossi, N. Rega, J. M. Millam, M. Klene, J. E. Knox, J. B. Cross, V. Bakken, C. Adamo, J. Jaramillo, R. Gomperts, R. E. Stratmann, O. Yazyev, A. J. Austin, R. Cammi, C. Pomelli, J. W. Ochterski, R. L. Martin, K. Morokuma, V. G. Zakrzewski, G. A. Voth, P. Salvador, J. J. Dannenberg, S. Dapprich, A. D. Daniels, Ö. Farkas, J. B. Foresman, J. V. Ortiz, J. Cioslowski, D. J. Fox, Gaussian Inc., Wallingford CT, **2009**.

[35] T. Ohta, H. Takaya, R. Noyori, *Inorg. Chem.* **1988**, *27*, 566 – 569.

Received: March 21, 2014
Published online on July 10, 2014

